Isotopomeric Conformational Changes in the Anisole−Water Complex: New Insights from HR-UV Spectroscopy and Theoretical Studies†

Massimiliano Pasquini,‡,§ Nicola Schiccheri,‡ Giovanni Piani,‡ Giangaetano Pietraperzia,*,‡,§ Maurizio Becucci,‡,§ Malgorzata Biczysko,*,|| Michele Pavone,|| and Vincenzo Barone||

LENS and Dipartimento di Chimica, Università di Firenze, via N. Carrara 1, Polo Scientifico, 50019 Sesto Fiorentino (FI), Italy, and Dipartimento di Chimica "Paolo Corradini" and CR-INSTM Village, Università di Napoli Federico II, Comp. Univ. M. S. Angelo, via Cintia, 80126 Napoli, Italy

Received: July 23, 2007; In Final Form: September 12, 2007

Resonance enhanced multiphoton ionization and rotationally resolved $S_1 \leftarrow S_0$ electronic spectra of the anisole−^2H_2O complex have been obtained. The experimental results are compared with high level quantum mechanical calculations and with data already available in the literature. Quite surprisingly, the equilibrium structure of the anisole−^2H_2O complex in the S_0 state shows some non-negligible differences from that of the isotopomer anisole−^1H_2O complex. Actually, the structure of the deuterated complex is more similar to the corresponding structure of the anisole−^1H_2O complex in the S_1 state. In anisole−water, two equivalent H(D) atoms exist as revealed by line splitting in the rotationally resolved spectra. It is possible to suggest a mechanism for the proton/deuteron exchange ruled by a bifurcated transition state for the exchange reaction, with both water hydrogen atoms interacting with the anisole oxygen atom. From the analysis of all of the available experimental data and of computational results, we can demonstrate that in the S_1 excited state the hydrogen bond in which the water molecule acts as an acid is weaker than in the electronic ground state but is still the principal interaction between water and the anisole molecules.

1. Introduction

Isotopic substitution of one or more atoms in a molecule is one of the most suitable tools to achieve the determination of the structure of unknown molecules. The success of this method relys on the assumption that isotopic substitution does not alter the fundamental nature of the interatomic interactions. However, it has been shown that this assumption is not always correct.[1,2] In a recent paper, Zhou et al. presented an NMR study on the crystal formed by the complex pentachlorophenol-4-methylpyridine. Upon substitution of the OH hydrogen atom with deuterium, a different crystal polymorph was stabilized. In a recent microwave spectroscopic study,[3] Giuliano and Caminati observed for the first time in the gas phase a change of the equilibrium structure upon isotopic substitution for the complex formed by anisole with ^1H_2O or ^2H_2O.

The anisole−water complex has attracted remarkable attention in the last years. The first study was carried out by experiments of resonance enhanced multiphoton ionization (REMPI) and IR-REMPI double resonance measurements combined with calculations at the MP2 level (MP2/aug-cc-pVDZ and MP2/6-31+G*).[4] A nonplanar equilibrium structure for the complex was predicted from the calculated stabilization energies and the comparison of experimental and theoretical OH vibrational frequencies. Then, our high-resolution laser induced fluorescence spectroscopy (LIF) measurement of the rotational constants for the complex containing ^1H_2O[5] showed how water is located in the anisole symmetry plane, with a conventional hydrogen bond in both the ground and the S_1 first singlet electronic excited states. Further microwave studies by Giuliano and Caminati[3] showed two different equilibrium positions for ^1H_2O and ^2H_2O in the ground state. They suggested a very flat, double well potential energy surface (PES) for the in-plane bending motion of water between the nearest hydrogen atom of the aromatic ring and a hydrogen atom of the methoxy group. Structural changes have been attributed to a different relative stability of the two minima caused by a slight variation of PES or substantial change in some of the low-frequency vibrational modes issuing from $^1H/^2H$ substitution. The presence of two equivalent and exchanging water hydrogen atoms in the system that leads to the doubling of the lines in the rotationally resolved spectra has been clearly pointed out. The authors suggested that, both hydrogen atoms point toward the oxygen atom of anisole forming a bifurcated H-bond. Very recently, a different geometry for the complex together with a two steps mechanism for the exchange of the two equivalent water protons has been proposed by Ribblett et al.[6] In this last work, the structure of the complex with the water molecule interacting through one of its hydrogen atoms with the oxygen atom of anisole (primary hydrogen bond) and through its oxygen atom with the ortho hydrogen of the aromatic ring (secondary interaction, weak H-bond) has been proposed for the S_0 ground state. The relative blue shift of the two subbands of the S_1-S_0 origin band leads the authors to suggest a change in the relative magnitude of these two interactions in the S_1 state. It has been shown that, although the total interaction between the two moieties becomes weaker upon photon absorption, the hydrogen bond in which the anisole molecule behaves as an acid becomes stronger in the S_1 state. The authors proposed that the bonding in which one of the ortho hydrogens of the aromatic ring interacts with the water oxygen atom becomes the main interaction in excited state (hydrogen bond

† Part of the "Giacinto Scoles Festschrift".

* Corresponding authors. E-mail: gianni.pietraperzia@unifi.it; malgorzata.biczysko@unina.it.

‡ LENS, Università di Firenze.

§ Dipartimento di Chimica, Università di Firenze.

|| Università di Napoli Federico II.

10.1021/jp0757558 CCC: $37.00
Published on Web 11/13/2007

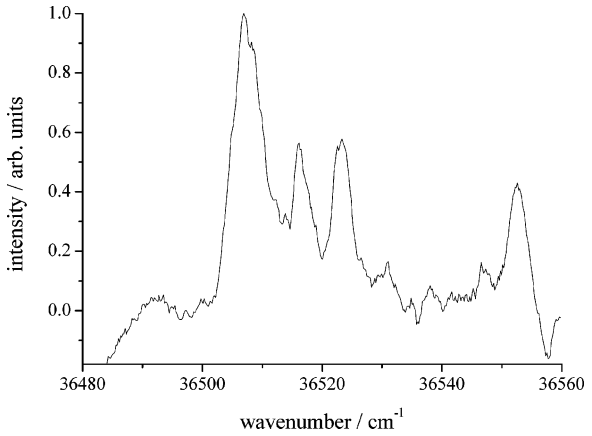

Figure 1. REMPI spectrum of the $S_1 \leftarrow S_0$ electronic transition of the anisole$-^2H_2O$ complex around the origin band.

switching). They also suggested that the mechanism for the hydrogen exchange corresponds to a two step combination of an inversion and a restricted internal rotation of water molecule.

It is quite evident that both the equilibrium geometry of this complex in the ground state and the mechanism for hydrogen exchange are not firmly established. In order to increase experimental information on this molecular complex, it seems to be very interesting to study anisole$-^2H_2O$ also in the first singlet excited electronic state S_1.

The complete set of experimental data that becomes now available together with quantum mechanical (QM) calculations performed in the present work provide new insights into unresolved issues about the structure and internal dynamics of the anisole−water complex in its ground and first excited electronic states.

2. Experimental Methods

The experimental methods for resonance-enhanced multiphoton ionization (REMPI) and high-resolution laser induced fluorescence spectroscopy (LIF) setups were described in detail elsewhere.[5,7] At first, we measured the REMPI spectrum for the anisole$-^2H_2O$ complex in order to locate the origin band of the $S_1 \leftarrow S_0$ electronic transition. ^2H_2O (99.9%) was purchased from Aldrich. Helium gas was allowed to flow through a reservoir which contains liquid ^2H_2O, and then the mixture was passed through another container with anisole. The two different containers were independently maintained at constant temperature (between −10 and +25 °C). The gas mixture so obtained was introduced in the molecular beam source and expanded in the high vacuum region. We used a solenoid pulsed valve (General Valve, series 9, 500 μ nozzle diameter) with a backing pressure of 400 kPa. A conical skimmer (Beam Dynamics mod. 2) selects the central part of the expansion and let the molecular beam to enter in the ionization region of the time-of-flight mass spectrometer. There the complex is at first ionized by the laser radiation and then it is accelerated and detected. The laser system used consists of a frequency doubled dye laser (Quanta System mod. D100), working on coumarin 153A (Radiant Dyes), pumped by the third harmonic of a Nd:YAG laser (Quanta System mod. SYL 201, 100 mJ per pulse at 355 nm, 10 Hz, 5 ns pulse duration). The origin band of the REMPI spectrum for the anisole-^2H_2O was readily located thanks to the previous knowledge of the spectroscopic properties of the anisole$-^1H_2O$. The REMPI spectrum obtained, reported in Figure 1, was assigned as discussed in section 4.2.

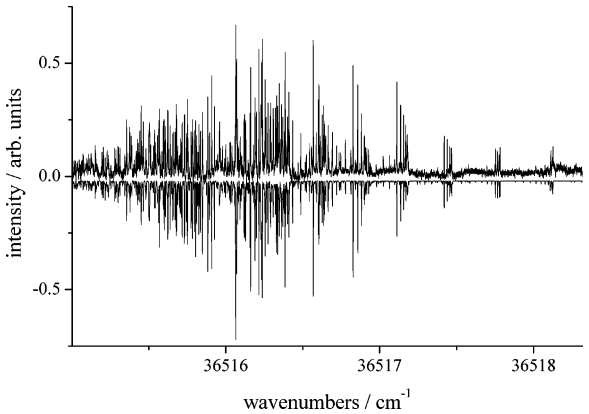

Figure 2. High-resolution LIF spectrum of the origin band of the $S_1 \leftarrow S_0$ electronic transition of the anisole$-^2H_2O$ complex. The experimental data are in the upper trace and the simulation based on the parameters of Table 1 in the lower trace.

The rotationally resolved spectrum of the origin band was then measured in a LIF experiment. The high-resolution experiment was performed with a continuous wave laser system based on a single mode, frequency stabilized, dye laser (Coherent Radiation 699−21) operating on pyrromethene 556 (Radiant Dyes), pumped by 6 W power at 515 nm, which delivered about 1.4 W power at 18 260 cm^{-1} on a 1 MHz bandwidth. Its emission was frequency doubled using a BBO crystal in a resonant optical cavity (LAS Wavetrain) generating up to 20 mW in the ultraviolet. A continuous molecular beam was produced allowing a gas mixture to expand through a 100 μm nozzle in a vacuum chamber and then selecting the core of the expansion by a 400 μm skimmer (Beam Dynamics mod. 2). The gas mixture contains vapors of ^2H_2O and anisole, in equilibrium with the respective liquids held at room temperature, and helium for a pressure of 300 kPa. The molecular beam was perpendicularly crossed with the UV laser beam and the resulting fluorescence emission was measured, by photon counting techniques, as a function of the excitation wavelength. The spectral resolution of this experiment is mainly limited by the residual Doppler broadening and can be described by a Gaussian function of 30 MHz FWHM. The frequency calibration was provided by the transmission fringes of a reference étalon. The rotationally resolved spectrum of the origin band of the complex consists of a single serie of transitions, and it was completely assigned with the *JB95* program by Plusquellic,[8] using a standard "S"-reduced Watson semirigid rotor Hamiltonian, see Figure 2. Once verified that the ground state level of the observed transition was the one reported in the microwave work,[3] the ground state combination differences method was used to further improve our frequency calibration, relying on the more accurate microwave data.

From the rotational constants, it was possible to derive the equilibrium position of the water molecule. We used a very simple model in which anisole is assumed to keep the same equilibrium structure of the isolated molecule also in the complex. The planar moments of inertia[9] are defined as

$$M_{aa} = \frac{1}{2}(-I_{xx} + I_{yy} + I_{zz}) = \sum_i m_i x_i^2$$

where I_{xx}, I_{yy} and I_{zz} are the eigenvalues of the inertia tensor. M_{aa} (and similarly M_{bb} and M_{cc} which can be derived with cyclic permutation of indexes) represents the distribution of masses out of the principal inertia planes *bc*. From the value of M_{cc}, it was immediately possible to show that the ^2H_2O molecule has

the center of mass in the anisole principal plane *ab* (which is also the anisole symmetry plane), as it was the case for the anisole−^1H_2O complex.[5] Then, using the Kraitchman equations,[10] it was possible to obtain, from the analysis of the inertia tensor, the distance r_{cm} between the center of mass of the two moieties and the angle θ between r_{cm} and the *b* inertia axis of the isolated anisole.

3. Computational Details

The ground state potential energy surface (PES) of the anisole−water complex was explored to test the hypothesis of different local minima for the anisole−^1H_2O and the anisole−^2H_2O, as proposed by Giuliano and Caminati.[3] The full geometry optimizations of the anisole−water 1:1 complex were performed with the B3LYP functional[11] starting from the several geometries with bifurcated $O^1H_2\cdots O$ and planar $O^1H\cdots O$ hydrogen-bond structures suggested by Giuliano and Caminati[3] and Ribblett et al.[6] Gaussian-type basis sets from 6-31G(d,p) to 6-311++G-(2d,2p) were exploited in order to test the effect of numerical approximations on the optimized structures: the use of a triple-ξ plus diffuse functions on heavy atoms is mandatory for achieving reliable geometrical parameters.

Several local minima of the anisole−water 1:1 complex in its ground and first singlet excited states were determined by full geometry optimizations at the B3LYP and TD-B3LYP[12] levels of theory, respectively. Besides, the anisole−water structure in the S_0 state was also computed at the MP2/6-311+G(d,p) level in order to resolve some ambiguities of former investigations based on second-order many-body perturbation theory.[4] For all of the optimized structures, zero-point vibrational energy (ZPVE) and the nature of stationary points were evaluated by harmonic frequency calculations for both anisole-^1H_2O and anisole-^2H_2O complexes; in the case of the ground state equilibrium structure, anharmonic effects were taken into account by a second-order perturbative scheme.[13] The ground state PES along the water−anisole in-plane bending coordinate, for bifurcated $OH_2\cdots O$ and/or planar $OH\cdots O$ structures, was explored by energy scan and constrained angle (O9O7C1 and/or dihedrals relative to water hydrogens) geometry optimization, followed by harmonic frequency calculations at each stationary point. Once again, the isotopic substitution was taken into account in order to obtain anisole−^1H_2O and anisole−^2H_2O ZPVE corrected profiles. Possible schemes of hydrogen exchange were studied by unconstrained transition state optimizations, and then we carried out intrinsic reaction path (IRC) calculations[14] and potential energy scans along approximate reaction coordinates. For the first excited electronic state, we performed a potential-energy scan along the O9O7C1 angle at the TD-B3LYP level, with all other geometry parameters constrained to their values at the S_1 minimum structure. All of these calculations were carried out with a locally modified version of Gaussian package.[15] Additionally, the energies of all of the found structural minima were refined by single-point energies computed at the coupled cluster level, including single double and (noniterative) triple excitations (CCSD(T)),[17,18] for the ground state, and at the equation-of-motion coupled cluster singles and doubles (EOM-CCSD)[19] level in the case of the S_1 excited state. For these post-Hartree−Fock calculations, we employed the MOLPRO[16] package. Concerning interaction energies and selected geometry optimizations in the ground state, the basis-set superposition error (BSSE)[20] was taken into account via the counterpoise (CP) correction scheme; CCSD and CCSD-(T) energies were corrected for the BSSE as evaluated at the MP2 level. In the case of the excited state, interaction energies and BSSE corrections were computed assuming the excitation to be localized onto the anisole molecule, in particular the CP corrected binding energies were calculated according to the scheme

$$\Delta E^*_{CP}(AW) = [E^{AW}_{AW}(AW)^* - E^{A}_{A}(A)^* - E^{W}_{W}(W)] + [E^{A}_{AW}(A)^* + E^{W}_{AW}(W) - E^{AW}_{AW}(A)^* - E^{AW}_{AW}(W)]$$

where $E^Y_X(Z)$ is the energy of subsystem *Z* at geometry *X* with basis set *Y*, A and W correspond to anisole and water molecule/basis-set respectively, excited-state calculations are labeled by an asterisk (*).

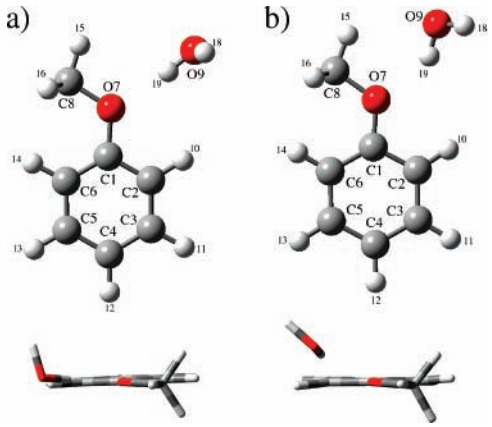

Figure 3. Geometry of the anisole−water OH···O complex in (a) the ground and (b) first singlet excited state.

4. Results and Discussion

As mentioned in the introduction, the structure of the anisole−water complex has been a matter of discussion in the past few years. Here, we present the results obtained from a combined experimental and theoretical approach, as it has been recently succesfully exploited for the anisole−ammonia 1:1 complex.[23]

Thus, for what concerns the anisole−water molecular complex in its ground and first singlet excited electronic states, extensive theoretical calculations have been performed to gain further insights into peculiar aspects of the experimental results and open issues, namely: (1) equilibrium geometry of complex in both electronic states; (2) blue shift of 0^0_0 $S_1 \leftarrow S_0$ band with respect to the isolated anisole; (3) splitting of the rovibronic lines attributed to the equivalence of water hydrogens (both ^1H and ^2H); (4) different ground state structure for anisole complex with ^1H_2O and ^2H_2O; (5) hydrogen bond switching in the S_1 electronic state.

4.1. Ground and Excited-State Geometry Structures. The structure and labeling of the anisole−water 1:1 molecular complex are sketched in Figure 3.

Table 1 lists the rotational constants, the determined centrifugal distortion constants and planar moments of inertia for the anisole−^2H_2O complex, as result from the fit of 503 assigned transitions (13 MHz standard deviation) in the HR-LIF spectrum of the origin band of the $S_1 \leftarrow S_0$ transition. The inspection of moments of inertia shows that the anisole−^2H_2O 1:1 complex is planar in its ground state and remains planar upon electronic excitation to the first singlet excited state S_1.

Regarding the theoretical determination of the anisole−water equilibrium structure, in order to achieve reliable geometrical parameters without losing computational feasibility, we performed a series of calculations, within the framework of density functional theory (DFT), by using different basis sets: resulting

TABLE 1: Rotational Constants, Centrifugal Distortion Constants (units cm^{-1}), and Planar Moments of Inertia (units amu $Å^2$) for the Anisole$-^2H_2O$ Complex as Determined by the Fit of 503 Assigned Transitions (13 MHz Standard Deviation) in the HR-LIF Spectrum of the Origin Band of the $S_1 \leftarrow S_0$ Transition[a]

	S_0	S_1
A	0.08874936(3)	0.100693(3)
B	0.03049311(2)	0.027190(1)
C	0.02291887(1)	0.021589(1)
D_J	$0.1504(1)\ 10^{-6}$	$0.030(3) \times 10^{-6}$
D_{JK}	$-1.81(2)\ 10^{-6}$	$-0.55(3) \times 10^{-6}$
D_K	$6.75(1) \times 10^{-6}$	$1.17(7) \times 10^{-6}$
d_1	$-6.147(7) \times 10^{-8}$	not determined
d_2	$-2.17(7) \times 10^{-9}$	not determined
M_{aa}	549.21(1)	616.7(1)
M_{bb}	186.32(1)	164.1(1)
M_{cc}	3.62(1)	3.3(1)

[a] The ground state constants and their associated errors are taken from ref 3.

geometrical parameters are listed in Table 2. These results show that the final geometry of the complex is quite sensitive to the choice of the basis set, e.g., in the case of the 6-311G(d,p), we found two different local minima, because the BSSE could lead to artifacts along the PES. Nevertheless, the medium-size 6-311+G(d,p) basis set, that includes diffuse functions on heavy atoms, provided sufficiently converged results, and therefore, it was selected for all of the calculations reported here.

Moreover, as reported by Table 2, the B3LYP density functional led always to a planar equilibrium structure, see the O9O7C1C2 dihedral, in qualitative agreement with recents experiments.[3,5,6]

On the contrary, earlier theoretical results at the MP2/6-31+G* [4] level of theory predicted a nonplanar structure for the anisole−water complex, in striking contrast with current experimental evidence. Moreover, the geometry optimization at the MP2 level with a larger basis set (6-311+G(d,p)) led also to a nonplanar equilibrium geometry. Thus, in order to further investigate such issue, full geometry optimization on the MP2/6-311+G(d,p) counterpoise-corrected potential energy surface ($MP2_{CP}$) was performed, and selected geometrical parameters are listed in Table 3. The calculation now converged to a planar structure, similar to those obtained by DFT calculations. Comparison of the relative energies, as listed in Table 3, shows that single-point energy calculations at both MP2 and CCSD(T) levels predicted the nonplanar structure to be favorite, and the stability order is reversed when BSSE correction is applied. This is the core of the problem behind the failures of standard MP2 calculations for the anisole−water complex. It is worth noting that the counterpoise corrected geometry optimization performed at a DFT level did not change the aforementioned structures nor did calculations with a semiempirical dispersion correction applied to the B3LYP density functional.[21,22] Thus, when DFT and MP2 calculations lead to significantly different structures, the source of error should not be found only in the well-known lack of dispersion forces by DFT-based approaches[23] but also in the significant BSSE that affects MP2 calculations.

In order to find local minima structures of the anisole−water 1:1 complex in its ground and excited states, we started from geometries already proposed in recent literature[3−6] for this system and from those reported for the similar anisole−ammonia 1:1 complex.[23] Indeed, all analogous structures (see Figure 4) have been found. Figure 4 reports all of the structures of the minima; indeed, a close resemblance to the anisole−ammonia case was found. Four planar structures (hereafter H···O···H, O···HC_3, O···HC_5, and OH···O) are characterized by classic hydrogen bond interactions with the water molecule acting as an acceptor. The single nonplanar structure OH···π is stabilized by interaction between one of the water hydrogen atoms with the electronic density of aromatic ring. It is worth noting that the OH···π nonplanar structure shows significant differences from the MP2/6-311+G(d,p) optimized structure with nonplanar OH···O interaction (see Tables 3 and 4 for respective structures). Upon electronic excitation, the H···O···H geometry vanishes and only four stable local minima remain. Inspection of rotational constants and calculated interaction energies listed in Table 5 confirms that the most stable structure for anisole-water 1:1 complex in both electronic states is planar (OH···O). Electronic excitation lower the relative stability of OH···O structure in comparison to the nonplanar one, from 3 kJ mol^{-1} in the ground state to 2 kJ mol^{-1} in S_1. Moreover, also weakly bonded O···HC_{ring} structures are less stable in the S_1 state.

This result can be easily rationalized by the nature of the electronic excitation: transfer of the electron density from the anisole oxygen atom to the aromatic ring (see Table 7 for atomic charges in both electronic states). In the S_1 state, a new relevant interaction center becomes effective since electron density on the aromatic ring increases and it is diffused all above the ring. This tends to destabilize planar structures with water acting as a proton donor due to lower electron density on the anisole oxygen and water acting as a proton acceptor due to the increased electron density on the ring. Thus, the only structure which gains stability is a nonplanar OH···π one with water acting as a proton donor interacting with increased aromatic electron density. Inspection of OH···O and OH···π interaction energies from TD-B3LYP and EOM-CCSD calculations shows that the TD−DFT calculations reverse the stability order, because of their overestimation of interactions with aromatic electron density. The out of plane hydrogen atom of the water molecule interacts with this electron density and pulls the water out of plane. This leads to the significant (ΔO9O7C1C2 $\sim$28°) planarity loss for OH···O TD−DFT optimized structure that is not shown by the experimental data. Despite this discrepancy, the overall description of the geometry of the complex in the excited state is satisfactory (see Tables 8 and 9 and section 4.3).

4.2. Origin Band Shift. The vibronic spectrum of anisole−^2H_2O shows several resonances, like the one already measured for anisole−^1H_2O.[5] Therefore, the same assignment strategy was used. In order to sort out the contribution arising from the fragmentation of larger clusters, we have performed the experiment under different thermodynamical conditions. In particular we have changed the heavy water concentration in the gas mixture by varying the temperature of its container. It was then possible to assign the two bands located at 36 516 and 36 553 cm^{-1} as the origin band and a vibronic band of the $S_1 \leftarrow S_0$ transition for the anisole−^2H_2O 1:1 complex, and the band at 36507 cm^{-1} as due to the fragmentation of an higher cluster anisole−$(^2H_2O)_x$ ($x > 1$).

The observed 132 cm^{-1} blue shift of the origin band for the complex anisole−^2H_2O with respect to the isolated anisole[24] is consistent with the 124 cm^{-1} shift for the anisole−^1H_2O 1:1 complex.[5] For both isopotomers, the blue shift of the 0_0^0 band is related to the weaker bonding of the anisole−water 1:1 complex in the excited state. This agrees with the planar OH···O structures in both electronic states, which become less stable upon electronic excitation due to the electron density transfer from the anisole oxygen to the aromatic ring, as discussed above. This qualitative picture is confirmed by the QM calculations summarized in Table 6. Theoretical transition

TABLE 2: Selected Geometry Parameters (Bond Lengths in Å and Angles in Degrees) and Rotational Constants (in cm^{-1}) of Anisole−^1H_2O 1:1 Complex Calculated by the B3LYP Level with 6−31G(d,p), 6−31+G(d,p), 6−311G(d,p), 6−311+G(d,p), 6−311++G(d,p), and 6−311++(2d,2p) Basis Sets

parameter	6-31G(d,p)	6-31+G(d,p)	6-311G(d,p)/ geom1	6-311G(d,p)/ geom2	6-311+G(d,p)	6-311++G(d,p)	6-311++G(2d,2p)
r(O9O7)	2.941	2.908	2.890	2.932	2.910	2.910	2.937
r(O9C2)	3.375	3.899	4.451	3.396	3.929	3.932	3.950
r(O7H19)	1.999	1.939	2.020	1.996	1.945	1.944	1.974
r(O9H10)	2.473	3.148	3.868	2.503	3.180	3.183	3.196
r(O9H15)	3.825	3.316	2.588	3.789	3.285	3.280	3.312
(O9O7C1)	110.9	127.1	148.4	111.6	128.3	128.4	128.4
(O9O7C8)	130.6	113.6	92.3	129.5	112.7	112.6	112.9
(O9C2C1)	90.5	79.5	67.4	89.8	79.1	79.0	79.4
(O7H19O9)	163.1	174.3	148.8	162.1	173.7	173.7	173.5
(O18O9O7C1)	84.5	76.2	86.1	81.9	76.6	74.8	76.4
(O9O7C1C2)	−3.1	−10.2	−2.9	−3.8	−6.3	−5.9	−5.4
A	0.0771	0.0905	0.1111	0.0778	0.0903	0.0904	0.0902
B	0.0364	0.0313	0.0280	0.0362	0.0315	0.0315	0.0314
C	0.0249	0.0235	0.0225	0.0249	0.0236	0.0235	0.0235

TABLE 3: Selected Geometry Parameters (Bond Lengths in Å and Angles in Degrees) and Energies (in kJ mol^{-1}) of the Anisole−Water 1:1 Complex Calculated by MP2/ 6-311+G(d,p) Classic and Counterpoise Corrected Geometry Optimizations

parameter	MP2	$MP2_{CP}$	energy	$\Delta E(MP2-MP2_{CP})$
r(O9O7)	2.8777	2.9843	MP2	−1.36
(O9O7C1)	119.1	125.4	CCSD(T)	−1.01
(O18O9O7C1)	46.8	85.1	MP2+BSSE	1.77
(O9O7C1C2)	39.7	10.0	CCSD(T)+BSSE	2.12

energies slightly overestimate the experimental values, by 0.2 and 0.13 eV for TD-B3LYP and EOM-CCSD, respectively. A much better agreement is obtained for the frequency shift of the electronic transition of the complex with respect of the isolated anisole: for anisole−^1H_2O, the observed 124 cm^{-1} blue shift of the 0_0^0 $S_1 \leftarrow S_0$ band can be compared to the theoretical values of 290 and 93 cm^{-1}, at TD-B3LYP/B3LYP and EOM-CCSD/CCSD levels respectively. Isotopic ^2H_2O substitution increases observed shift to 132 cm^{-1}, to be compared with 306 and 108 cm^{-1} computed at density functional and coupled cluster levels, respectively. Weaker hydrogen bonding in the

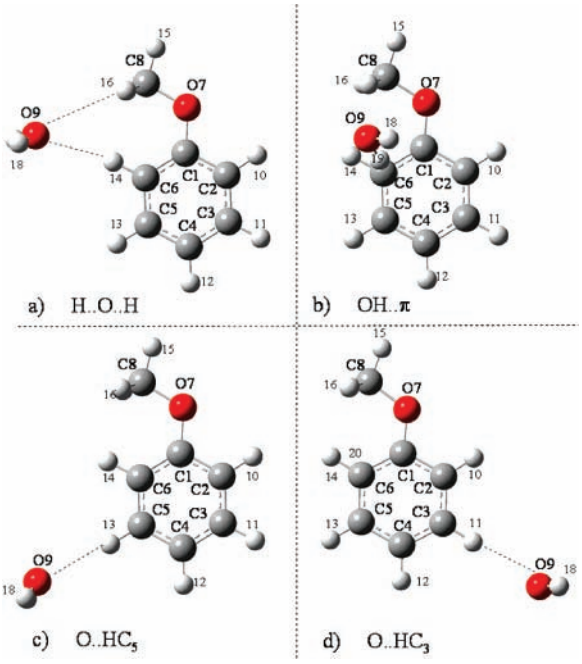

Figure 4. Calculated geometries for the other identified local minima in the ground state potential energy surface for the anisole−^1H_2O complex.

TABLE 4: Selected Geometry Parameters (Bond Lengths in Å and Angles in Degrees) of the Anisole−Water 1:1 Complex in Its Ground and Excited States[a]

structure	parameter	S_0	S_1	ΔS_1-S_0
OH···O	*r*(O9O7)	2.9104	2.9124	0.002
	r(O9C2)	3.9294	4.3215	0.392
	r(O7H19)	1.9451	2.0749	0.130
	r(O9H10)	3.1799	3.7791	0.599
	r(O9H15)	3.2851	2.7152	−0.570
	(O9O7C1)	128.3	140.8	12.5
	(O9O7C8)	112.7	93.7	−19.0
	(O9C2C1)	79.1	69.6	−9.5
	(O7H19O9)	173.7	144.0	−29.8
	(O18O7C1C2)	−76.6	−9.5	67.0
	(O9O7C1C2)	−6.3	−34.5	−28.2
H···π	*r*(O9H16)	2.6727	2.3627	−0.310
	r(O9O7)	3.7750	3.6743	−0.101
	r(O7H18)	4.2091	4.2570	0.048
	r(O7H19)	3.3551	3.2843	−0.071
	r(O9C8)	3.6129	3.3466	−0.266
	r(O9C1)	3.5785	3.5641	−0.014
	r(O9C6)	3.3049	3.2130	−0.092
	r(H19Cl)	2.8587	2.8628	0.004
	r(H19C6)	2.5040	2.3552	−0.149
	(O9H16C8)	143.7	149.0	5.3
	(O7H19O9)	108.6	106.1	−2.5
	(O9C8O7)	85.3	91.4	6.1
	(O9H19C1)	132.1	129.8	−2.3
	(O9H19C6)	140.3	146.8	6.5
	(O9O7C1C2)	−119.7	−126.1	−6.4
H···O···H	*r*(O7O9)	3.6608		
	r(O9H16)	3.1004		
	r(O9H14)	3.2106		
	r(O9C6)	3.5293		
	r(O9C8)	3.6608		
	(O9H14C6)	105.6		
	(O9H16C8)	112.5		
	(O9C8O7)	124.0		
	(O9C6C1)	126.9		
	(O9O7C1C2)	−178.3		
O···H−C_3	*r*(C3O9)	3.5	3.52	0.018
	r(O9H11)	2.42	2.44	0.021
	(O9H11C3)	178.8	178.3	−0.5
	(O9C3C2)	118.7	122.1	3.4
	(O9C3C4)	121.1	119.1	−2.0
	(O9C3C2C1)	180.0	180.0	0.0
O···H−C_5	*r*(C5O9)	3.51	3.53	0.018
	r(O9H13)	2.43	2.45	0.020
	(O9H13C5)	176.7	178.2	1.5
	(O9C5C6)	116.7	119.1	2.3
	(O9C5C4)	122.7	121.8	-0.9
	(O9C5C6C1)	180.0	180.0	0.0

[a] For S_0 values calculated at the B3LYP/6−311+G(d,p) level, for S_1 the TD-B3LYP/6−311+G(d,p) results.

TABLE 5: Properties of the Anisole−Water 1:1 Complex in Its Ground and First Excited Electronic State[a]

	S_0							
	rotational constants						interaction energy[b]	
	^1H_2O			^2H_2O				
	A	B	C	A	B	C	B3LYP	CCSD(T)[c]
OH···O	0.090345	0.031504	0.023555	0.088586	0.030281	0.022805	−10.14	−10.65
H···π	0.065342	0.038948	0.030737	0.062249	0.038256	0.029938	−4.50	−7.61
H···O···H	0.069085	0.033691	0.022821	0.067068	0.031640	0.021721	−2.08	−4.67
O···H−C_3	0.093309	0.023334	0.018782	0.091013	0.021782	0.017723	−0.55	−1.46
O···H−C_5	0.065603	0.027801	0.019653	0.064688	0.025708	0.018558	−0.47	−1.67
exp	0.098114	0.030009	0.023147	0.088749	0.030493	0.027193		
	S_1							
	rotational constants						interaction energy[b]	
	^1H_2O			^2H_2O				
	A	B	C	A	B	C	TD-B3LYP	EOM-CCSD[d]
OH···O	0.100166	0.028717	0.022854	0.100166	0.028717	0.022854	−6.67	−8.05
H···π	0.069119	0.037550	0.029880	0.069119	0.037550	0.029880	−10.36	−5.70
O···H−C_3	0.094796	0.022639	0.018386	0.094796	0.022639	0.018386	1.10	−0.12
O···H−C_5	0.065933	0.026921	0.019238	0.065933	0.026921	0.019238	0.57	−0.59
exp	0.103047	0.028271	0.022390	0.100692	0.027193	0.021600		

	$S_1 \leftarrow S_0$					
	^1H_2O			^2H_2O		
	TD-B3LYP	EOM-CCSD	exp	TD-B3LYP	EOM-CCSD	exp
transition/eV	4.735	4.658	4.526	4.737	4.660	4.527
shift/cm^{-1}	290	93	124	306	108	132
Δr_{cm} (S_1-S_0)/Å	0.159		0.127			

[a] Interaction energies in kJ mol^{-1} corrected for BSSE and ZPE (see text). Rotational constants in cm^{-1}. [b] All energies corrected for ZPE based on harmonic frequency calculations at DFT/TD-DFT levels, see text. [c] Energies from single-point calculations for B3LYP/6-311+G(d,p) optimized structures and corrected for BSSE at MP2/6-311+G(d,p) level, see text. [d] Energies from single-point calculations for TD-B3LYP/6-311+G(d,p) optimized structure.

TABLE 6: Atomic Charges from Natural Bond Orbital[25] Analysis for the Anisole−Water 1:1 Complex[a]

	natural charge		
atom	S_0	S_1	S_1-S_0
C1	0.381	0.482	0.101
C2	−0.255	−0.310	−0.055
C3	−0.152	−0.256	−0.103
C4	−0.238	−0.097	0.141
C5	−0.152	−0.253	−0.101
C6	−0.299	−0.335	−0.036
O7	−0.654	−0.621	0.032
C8	−0.103	−0.107	−0.005
O9	−0.949	−0.945	0.004
H10	0.213	0.208	−0.004
H11	0.197	0.200	0.003
H12	0.198	0.191	−0.007
H13	0.195	0.199	0.004
H14	0.202	0.204	0.002
H15	0.175	0.190	0.016
H16	0.148	0.153	0.005
H17	0.151	0.156	0.005
H18	0.452	0.457	0.006
H19	0.490	0.483	−0.007

[a] The S_0 values are calculated at the HF/6-311+G(d,p) level for the B3LYP/6-311+G(d,p) optimized structure; the S_1 values are calculated at the CIS/6-311+G(d,p) level for the TD-B3LYP/6-311+G(d,p) optimized structure.

excited S_1 state reflects also in the increase of the distance between the center of mass of anisole and water. From the rotational constants obtained by fitting the experimental spectrum with a semirigid Hamiltonian, it is possible to calculate the relative position of the anisole and water centers of mass (considering the water molecule as a rigid sphere). Table 8 shows a significant increase of r_{cm} for both isopotomers (about 0.13 Å for anisole−^1H_2O and 0.26 Å for anisole−^2H_2O). Theoretical geometries show the same tendency, the distance between centers of mass increasing by 0.159 Å from the equilibrium distance (4.360 Å) in the ground state (see Table 6).

TABLE 7: Geometry of the Anisole−Water Complex as Derived from the Analysis of the Experimental Data[a]

	^1H_2O	^2H_2O
	S_0	
r	4.483(2)	4.343(1)
θ	46.6(1)	41.6(1)
ϕ	5.5(1)	8.1(1)
	S_1	
r	4.611(3)	4.590(3)
θ	51.7(1)	51.0(1)
ϕ	7.0(1)	6.8(1)

[a] The position of the water center of mass is defined with respect to the anisole principal inertia axes: r is the distance between the two centers of mass, θ is the angle between the projection of r on the anisole ab plane and the anisole b inertia axis, and ϕ is the elevation angle of r with respect to the anisole ab plane. Units are Å and degrees.

TABLE 8: Selected Geometric Parameters for the Anisole−^1H_2O(−^2H_2O) Complex Obtained with a Combined Experimental and Theoretical Method[a]

	^1H_2O		^2H_2O	
	S_0	S_1	S_0	S_1
O9H15	3.03	2.70	3.29	2.74
O9H10	3.43	3.74	3.13	3.69
O7H19	1.94	1.94	2.07	2.07
O9O7	2.88	2.94	2.88	2.93
C2C1O7O9	−12.24	−17.17	−15.33	−16.35

[a] See section 4.5. Distances are in Å and angles in degrees.

TABLE 9: Relative Energies and Rotational Contants for Global Minimum of the Anisole−Water Complex from B3LYP/6-311+G(d,p) Geometry Optimization, and Local Minima along O9O7C1 PES Best Fitting Experimental Rotational Constants of Anisole−^1H_2O and Anisole−^2H_2O[a]

	opt-B3LYP	OOC = 128	OOC = 136	exp
(O9O7C1)	128.29	128.00	136.00	
		Energies		
CCSD(T)	0.00	−0.12	0.04	
+BSSE	0.00	0.02	0.05	
+ZPE(^1H_2O)	0.00	−0.07	0.04	
+ZPE(^2H_2O)	0.00	−0.07	0.03	
		Rotational Constants Anisole−^1H_2O		
A	0.090345	0.090059	0.097319	0.098114
B	0.031504	0.031537	0.029963	0.030009
C	0.023555	0.023615	0.023102	0.023147
		Rotational Constants Anisole−^2H_2O		
A	0.088586	0.088238	0.095225	0.088749
B	0.030282	0.030325	0.028804	0.030493
C	0.022805	0.022870	0.022340	0.027193

[a] See the text for details. Energies in kJ mol^{-1} calculated at the CCSD(T) level, with basis-set corrections (BSSE) from MP2/6-311+G(d,p) calculations, and corrected for zero-point energy (ZPE) from harmonic frequency calculations at the B3LYP/6-311+G(d,p) level. Units: angles in degrees and rotational constants in cm^{-1}. Experimental data for Anisole−^1H_2O from ref 5 and for anisole−^2H_2O from ref 3.

4.3. Splitting in the Rotational/Rovibronic Transitions. The origin band of the $S_1 \leftarrow S_0$ transition for the 1:1 anisole−^1H_2O complex, presents a splitting attributed to the exchange of two equivalent hydrogen atoms.[5,6] The LIF spectra of the 1:1 anisole−^2H_2O complex from this work show only a single component for the same band. The experimental high-resolution spectrum and its simulation performed using the data reported in Table 1 are shown in Figure 2. On the other hand, ground-state results by Giuliano and Caminati[3] have shown that the two sub-bands correspond to the exchange of two equivalent ^2H. From the values reported for both isotopomers it is evident that the differences between the rotational constants for the two sub-bands of anisole−^2H_2O are one order of magnitude smaller with respect to the anisole−^1H_2O complex. Thus the splitting of the LIF band origin of anisole−^2H_2O complex, if present, could possibly be smaller than our spectral resolution. The doubling of the lines in the rotationally resolved spectra is a fingermark for the two equivalent water hydrogen atoms in the system. Two different mechanisms have been proposed to explain their presence: Giuliano and Caminati[3] suggested a structure with both hydrogen atoms of the water molecule pointing toward the oxygen atom of anisole forming a bifurcated H-bond; the other possibility is related to an intermolecular dynamics of the complex leading to the exchange of water hydrogen atoms, for which Ribblett et al.[6] proposed a two step mechanism. QM calculations at the B3LYP/6-311+G(d,p) level give new insights about the origins of the experimentally observed splitting. A search for the bifurcated structure of the complex has been performed by constrained geometry optimizations (O7O9C1 angle and dihedrals related to the position of water hydrogens fixed), and all the found stationary points showed one imaginary frequency. Moreover, unconstrained transition state (TS) optimizations led to the same $OH_2\cdots O$ structure. On the other hand, for all of the tested bending angles (O9O7C1), the local minimum with classical hydrogen-bonded OH···O structure has been found. Panel a of Figure 5 shows the H-bonded planar minimum and bifurcated transition state structures, along with related (MIN and TS) potential energy paths for the in-plane bending motion of water. The planar

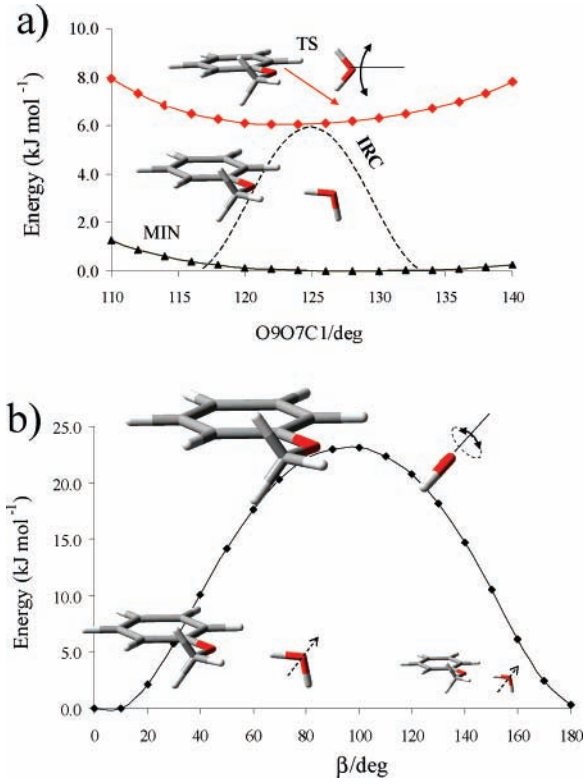

Figure 5. Equivalence of water hydrogens in the ground electronic state of the anisole-water complex. (a) Hydrogen-bonded vs bifurcated structure: minimum (MIN) and transition state (TS) potential energy paths along O9O7C1 angle; planar H-bonded structures black line and triangles, bifurcated structures red line and diamonds. Energies from constrained geometry optimizations at B3LYP/6-311+G(d,p) level, symbols correspond to stationary points. Bifurcated to linear H-Bonded reaction path (dashed lines) as calculated by IRC-B3LYP/6-311+G-(d,p), see text. (b) Hydrogen exchange by internal rotation of water, potential energy scan along the bisector axis. All energies is kJ mol^{-1}.

OH···O geometries are more stable than the TS bifurcated ones irrespective of the O9O7C1 angle. The reaction path characterized by means of intrinsic reaction coordinate (IRC) calculations is also shown. It confirms that the bifurcated structure is indeed the transition state connecting two equivalent planar H-bonded structures with a barrier of only ∼6 kJ mol^{-1}. The two step mechanism for hydrogen exchange is related to the internal rotation of the water molecule and can be explored by potential energy scans along the water bisector axis (see panel b of Figure 5). The resulting barrier of about 23 kJ mol^{-1} is almost four times larger than that predicted by the reaction path calculations. Thus, the out-of-plane rotation of the water molecule, ruled by the bifurcated transition state, seems to be the favored mechanism for the exchange of two equivalent hydrogen atoms. The splitting for the anisole−^2H_2O is an order of magnitude lower than for the lighter isotopomer, thus suggesting that tunneling may play an important role in exchange dynamics. The difference between the two isopotomers can be also attributed to some loss of planarity in the anisole−^2H_2O with respect to the anisole−^1H_2O (see angle ϕ from Table 7 and angle C2C2O7O9 in Table 8), which should result in a nonequivalence of the water hydrogen atoms. The exchange of protons is a clear signature of the flexibility of this complex. Other large amplitude motions are possibly relevant for the complete description of its internal dynamics. An example is the rotation of the water molecule around the O9−H19 axis that by a 180° rotation will lead to an equivalent geometry of the complex (but not to an

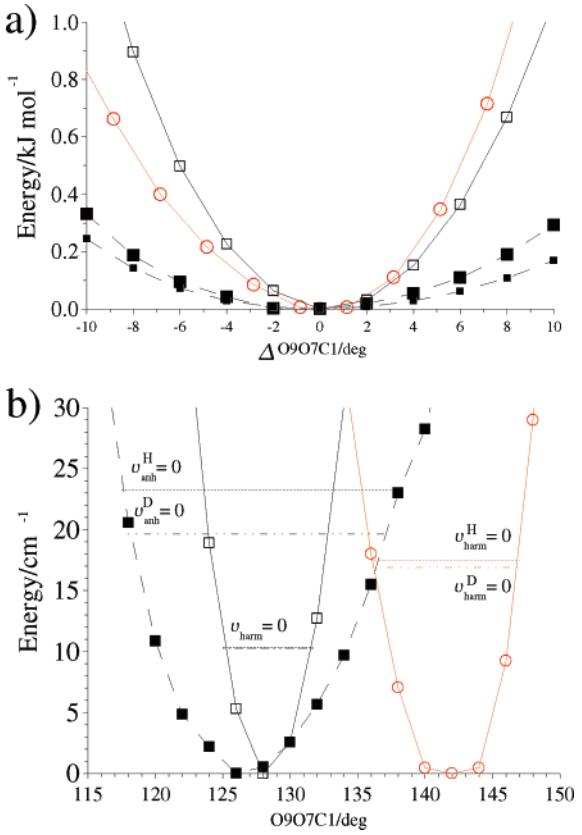

Figure 6. Potential energy scan and first ($\upsilon = 0$) vibrational levels along the in-plane bending of water (O9O7C1 angle) for anisole-water complex in ground and excited states. S_0 solid lines and squares, S_1 solid lines and circles; unrelaxed scan solid lines and open symbols, relaxed scan dashed lines and filled symbols (for S_0 larger symbols correspond to ZPE corrected energies). For ground state B3LYP/6-311+G(d,p) and for excited state TD-B3LYP/6-311+G(d,p) values. Panel a) position relative to the global minimum of 128.3° (S_0) and 140.8° (S_1), energies in kJ mol^{-1}; panel b) absolute values of O9O7C1 angle, energies in cm^{-1}. All energies relative to the S_0 and S_1 minimum energy structures.

exchange of the water hydrogen atoms). The barrier for this motion is ~4 kJ mol^{-1}.

4.4. Structural Isotopic Effect. Giuliano and Caminati[3] showed that the anisole−water 1:1 complex in its ground state is characterized by the change of geometry structure upon ^{1}H/^{2}H isotopic substitution in H_2O. In the present work, the structure of the anisole−^2H_2O 1:1 complex in its first singlet excited state S_1 has been determined for the first time. Table 8 lists the geometrical parameters for the relative position of the anisole and water centers of mass obtained from the experimental rotational constants (the experimental data for isolated anisole and anisole−^1H_2O are taken from refs 24 and 5). The intermolecular distances we calculated for anisole−^1H_2O are in agreement with those presented by Ribblett et al. within the experimental error.[6] In the S_1 excited state, anisole−^1H_2O and anisole−^2H_2O have almost identical structures, which are, in turn, very close to the geometry of anisole−^1H_2O in the S_0 state. Thus, the structural isotopic effect in the anisole−water 1:1 complex is not present in the excited-state, and it should be only attributed to the ground state. As already mentioned in section 4.3, it is possible to identify several OH···O hydrogen-bonded local minima (all vibrational frequencies positive) along O9O7C1 angle. Subsequent frequency calculations allowed to obtain the ZPVE corrected anisole−^1H_2O and anisole−^2H_2O energy profiles. From panel a) of Figure 6, it is evident that for the relaxed scan ±10° angle variations do change energy by less than 0.3 kJ mol^{-1} and the ZPVE correction increases this value by only about 0.1 kJ mol^{-1}. The ZPVE(^1H_2O) and ZPVE-(^2H_2O) corrected profiles are indistinguishable on the plot. Therefore, only one set of data is reported. Post-HF correlated calculations confirm minor variations of the potential energy surface for the in-plane bending motion of water. Table 9 lists the single-point CCSD(T)/6-311+G(d,p), BSSE, and ZPVE corrected energies computed on the B3LYP optimized global minimum and on two structures extracted from constrained geometry optimizations for obtaining rotational constants that best fit the experimental values for the anisole−^1H_2O or the anisole−^2H_2O. The structure with O9O7C1 = 136° (giving the best match with experimental data for anisole−^1H_2O) is only about 0.1 kJ mol^{-1} less stable than the structure O9O7C1 = 128° (giving the best fit with the anisole−^2H_2O data). The relative stability remains almost unchanged if zero-point energy corrections are included for both isotopes. QM calculations show an extremely flat PES and the presence of many local minima rather than the double well potential postulated by Giuliano and Caminati.[3] Calculated ground state global minimum for the anisole−water 1:1 complex agrees well with the experimental structure of anisole−^2H_2O. It is possible that slightly different geometry for structure with lighter isopotomers might be associated to the isotopic dynamic effects on the relative position of water moiety. Panel b) of Figure 6 shows harmonic and anharmonic potential energy profiles along O9O7C1 coordinate together with the corresponding zero point vibrational levels for both isotopomers. It can be found that in the first vibrational level ($\upsilon = 0$) the O9O7C1 angle can vary from about 118° to 138° for the anisole−^1H_2O, and slightly less for anisole−^2H_2O. Moreover, the vibrationally averaged position of water molecule is slightly shifted toward one of the methyl hydrogens for the lighter isotopomer. Such findings are in qualitative agreement with the observed geometry change, but the magnitude of the shift (~0.5°) is much smaller than that deduced from the experiment. It is possible that in order to reproduce the experimental isotopic structural effect it is necessary to perform BSSE-free optimizations at highly correlated levels, add higher order corrections for anharmonicity, or include explicitly dynamic effects, which has not been tested in this work. There remains to explain why only a single global minimum for both isotopic species has been observed in the first excited electronic state. The calculated unrelaxed TD-B3LYP potential energy profile is similar to the corresponding ground state B3LYP unrelaxed scan (see Figure 6). Angle variations of ±10° from the equilibrium value resulted in rising the energy up to ~1 kJ mol^{-1}. Zero-point vibrational levels calculated at the harmonic level show larger differences betwen both isotopes in the S_1 state, as harmonic $\upsilon^H = 0$ and $\upsilon^D = 0$ levels are distinguishable for the excited state. This contradiction most likely needs to be attributed to the overestimation of the planarity loss for TD-B3LYP optimized geometry, as already pointed out in section 4.1. Thus the true shape of potential energy profile along O9O7C1 in the first excited-state might not be as flat as the one shown in Figure 6. A possible explanation may arise from the atomic charges reported in Table 7. With the electronic excitation it is predicted an increase of charge on the H15 atom and a decrease on H10. Thus the geometry with the water closer to the methyl group may become more stabilized.

4.5. S_0−S_1 Hydrogen Bond Switching. The relative positions of the anisole and water atoms for anisole−^1H_2O and anisole−^2H_2O complexes in ground and excited electronic states have been obtained combining the experimental and QM results. Our best theoretical complex structure from B3LYP/6-311+G(d,p)

calculations for S_0 and TD-B3LYP/6-311+G(d,p) for S_1 has been combined with the experimentally obtained rotational constants. In particular it is possible to obtain the distance between the atoms of the anisole molecule and the center of mass of the water molecule, which is assumed to coincide with the oxygen atom position. Selected intermolecular parameters are listed in Table 9; for the O7H19 value, we used the QM-calculated one. It is evident that in both states the complex is primarily bonded by the interaction between the water hydrogen and the oxygen atom of the anisole, as indicated by the O7H19 and the O7O9 distances. In the S_0 state the O···H distances related to the secondary interactions O9H15 and O9H10 are very similar. The water oxygen atom is placed in the middle between the methyl group and the nearest ortho hydrogen atom of the aromatic ring. In the S_1 state, the bonding distance related to the principal hydrogen bond increases, in line with the nature of the electronic transition involved, as previously discussed. The main structural change is related to the secondary interactions which are no more balanced. Upon electronic excitation the O9H15 distance decreases and the O9H10 distance increases by about 0.3 Å; the secondary interaction is now clearly the one between one of the methyl hydrogen atoms and the water oxygen atom. This finding is confirmed on inspection of the atomic charges listed in Table 7. Anisole oxygen loses electron density which is transferred to the aromatic ring, and due to the weaker OH···O bond, some electron density is transferred back to the H19. Regarding hydrogen atoms involved in the secondary interaction, there is no significant charge difference for the ortho hydrogen, whereas the methyl hydrogen H15 becomes more positive indicating a stronger interaction than in the ground state with water oxygen. Thus, although the total binding interaction becomes weaker in the excited state, the hydrogen bond in which water acts as a base becomes relatively stronger. These findings are in perfect agreement with the experimental data reported by Ribblett et al.[6] but not with their suggestion about hydrogen bond switching. Our results show that the hydrogen bond OH···O, in which water acts as an acid, remains the primary interaction in both states. Moreover the hydrogen bond between water oxygen and methyl hydrogen (not ortho hydrogen from the aromatic ring) is the one gaining strength upon electronic excitation.

5. Conclusions

The high-resolution electronic spectrum of the origin band of the $S_1 \leftarrow S_0$ transition for the anisole−^2H_2O complex has been observed and assigned for the first time. Within our spectral resolution (30 MHz) there is no evidence of splitting of the rovibronic lines. Two series of transitions were observed in the rotational spectrum of this complex by Giuliano and Caminati.[3] From a comparison with high level quantum mechanical calculations, it was possible to obtain detailed information about the geometry of the complex in both electronic states. In the S_0, state the equilibrium structure is different from the corresponding structure for the anisole−^1H_2O complex. The deuterated water molecule is placed nearer to the ortho hydrogen of the aromatic ring. The ground state experimental structure of anisole−^2H_2O complex agrees well with the theoretical B3LYP/6-311+G(d,p) structure. In the S_1 state, the deuterated water molecule moves toward the methyl hydrogen atom with an angular displacement of about 10°. For both of the anisole−water isotopomers the strongest interaction is always the H-bond formed between one of the water $^1H/^2H$ atoms and the anisole oxygen. This bond is weaker in the S_1 excited state, thus explaining the blue shift of the origin band of the complex with respect to the corresponding band of the anisole bare molecule. Secondary interactions between the water oxygen atom and the hydrogen atoms of the anisole molecule are responsible for the water position along O9O7C1 angle. In the electronic ground state the ^2H_2O molecule is placed more or less in the middle between the nearest ortho hydrogen of the aromatic ring and the nearest hydrogen atom of the methyl group, whereas the ^1H_2O molecule is slightly displaced toward the nearest methyl hydrogen (see Table 9). In the S_1 state, both ^1H_2O and ^2H_2O are clearly displaced toward the methyl group. For proton/deuteron exchange in the anisole−water complex, a mechanism involving an out-of-plane rotation of water molecule with a bifurcated transition state structure is proposed based on the reaction path following calculations at the B3LYP/6-311+G(d,p) level. An alternative mechanism related to restricted internal rotation has been found to be much less favorable.

Acknowledgment. This work was supported by Italian MIUR and by the EU (under Contract No. RII3-CT-2003-506350). The large scale computer facilities of the VILLAGE network (htttp://village.unina.it) are also kindly acknowledged. M.B. is grateful to the Wroclaw Centre for Networking and Supercomputing for access to the MOLPRO code and related computer time.

References and Notes

(1) Ubbelohde, A. R.; Gallagher, K. J. *Acta Crystallogr.* **1995**, *8*, 71.
(2) Zhou, J.; Kye, Y.-S.; Harbison, G. S. *J. Am. Chem. Soc.* **2004**, *126*, 8392.
(3) Giuliano, B. M.; Caminati, W. *Angew. Chem., Int. Ed.* **2004**, *44*, 603.
(4) Reimann, B.; Buchold, K.; Barth, H. D.; Brutschy, B.; Tarakeshwar, P.; Kim, K. S. *J. Chem. Phys.* **2002**, *117*, 8805.
(5) Becucci, M.; Pietraperzia, G.; Pasquini, M.; Piani, G.; Zoppi, A.; Chelli, R.; Castellucci, E.; Demtroeder, W. *J. Chem. Phys.* **2004**, *120*, 5601.
(6) Ribblett, J. W.; Sinclair, W. E.; Borst, D. R.; Yi, Y. T.; Pratt, D. W. *J. Phys. Chem. A* **2006**, *110*, 1478.
(7) Kerstel, E. R. Th.; Becucci, M.; Pietraperzia, G.; Castellucci, E. *Chem. Phys.* **1995**, *199*, 263.
(8) Plusquellic, D. F. http://physics.nist.gov/Divisions/Div844/facilities/uvs/jb95userguide.htm; NIST: Gaithersburg, MD, 2003.
(9) Gordy, W.; Cook, R. L. *Microwave Molecular Spectra*, 3rd ed.; Wiley: New York, 1984.
(10) Kraitchman, J. *Am. J. Phys.* **1953**, *21*, 17.
(11) A description of basis sets and standard computational methods can be found in Foresman, J. B.; A. F. V. *Exploring Chemistry with Electronic Structure Methods*, 2nd ed.; Gaussian, Inc.: Pittsburgh, PA, 1996.
(12) Scalmani, G.; Frish, M. J.; Menucci, B.; Tomasi, J.; Cammi, R.; Barone, V. *J. Chem. Phys.* **2006** *124*, 094107.
(13) Barone, V. *J. Chem. Phys.* **2005** *122*, 014108.
(14) Gonzalez, C.; Schlegel, H. B. *J. Phys. Chem.* **1990**, *94*, 5523.
(15) Frisch et al.; *Gaussian Development Version*, revision F.01; Gaussian, Inc.: Wallingford, CT, 2006.
(16) Werner, H.-J.; Knowles, P. J.; Lindh, R.; Manby, F. R.; Schütz, M.; Celani, P.; Korona, T.; Rauhut, G.; Amos, R. D.; Bernhardsson, A.; Berning, A.; Cooper, D. L.; Deegan, M. J. O.; Dobbyn, A. J.; Eckert, F.; Hampel, C.; Hetzer, G.; Lloyd, A. W.; McNicholas, S. J.; Meyer, W.; Mura, M. E.; Nicklass, A.; Palmieri, P.; Pitzer, R.; Schumann, U.; Stoll, H.; Stone, A. J.; Tarroni, R.; Thorsteinsson, T. *Molpro*, version 2006.1, a package of ab initio programs, 2006. see http://www.molpro.net.
(17) Hampel, C.; Peterson, K. A.; Werner, H. J. *Chem. Phys. Lett.* **1992**, *190*, 1.
(18) Deegan, M. J. O.; Knowles, P. J. *Chem. Phys. Lett.* **1994**, *227*, 321.
(19) Korona, T.; Werner, H.-J. *J. Chem. Phys.* **2003**, *118*, 300.
(20) Simon, S.; Duran, M.; Dannenberg, J. J. *J. Chem. Phys.* **1996**, *105*, 11024.
(21) Grimme, S. *J. Comput. Chem.* **2006**, *27*, 1787.
(22) Barone, V.; Pavone, M. To be published.
(23) Biczysko, M.; Piani, G.; Pasquini, M.; Schiccheri, N.; Pietraperzia, G.; Becucci, M; Pavone, M.; Barone, V. *J. Chem. Phys.* In press.
(24) Eisenhardt, C. G.; Pietraperzia, G.; Becucci, M. *Phys. Chem. Chem. Phys.* **2001**, *3*, 1407.
(25) Reed, A. E.; Curtiss, L. A.; Weinhold, F. *Chem. Rev.* **1988**, *88*, 899.